Inhibition of topoisomerase IIα and G_2 cell cycle arrest by NK314, a novel benzo[*c*]phenanthridine currently in clinical trials

Lei Guo,[1,2] Xiaojun Liu,[1] Kiyohiro Nishikawa,[3] and William Plunkett[1,2]

[1]Department of Experimental Therapeutics, The University of Texas M. D. Anderson Cancer Center; [2]The University of Texas Graduate School of Biomedical Sciences at Houston, Houston, Texas; and [3]Nippon Kayaku Co. Ltd., Tokyo, Japan

Abstract

NK314 is a novel synthetic benzo[*c*]phenanthridine alkaloid that has recently entered clinical trials as an antitumor compound, based on impressive activities in preclinical models. The present investigations were directed at determining the mechanism of action of this agent. NK314 induced significant G_2 cell cycle arrest in several cell lines, independent of p53 status, suggesting the existence of a common mechanism of checkpoint activation. The Chk1-Cdc25C-Cdk1 G_2 checkpoint pathway was activated in response to 100 nmol/L NK314 in ML-1 human acute myeloid leukemia cells. This was associated with the phosphorylation of the histone variant H2AX, an action that was predominant in the G_2 population, suggesting that double-strand DNA breaks caused cells to activate the checkpoint pathway. Double-strand DNA breaks were visualized as chromosomal aberrations when the G_2 checkpoint was abrogated by 7-hydroxystaurosporine. *In vitro* assays showed that NK314 inhibited the ability of topoisomerase IIα to relax supercoiled DNA and trapped topoisomerase IIα in its cleavage complex intermediate. CEM/VM1 cells, which are resistant to etoposide due to mutations in topoisomerase IIα, were cross-resistant to NK314. However, CEM/C2 cells, which are resistant to camptothecin due to mutations in topoisomerase I, retained sensitivity. These findings support the conclusion that the major mechanism of NK314 is to inhibit topoisomerase IIα, an action that leads to the generation of double-strand DNA breaks, which activate the G_2 DNA damage checkpoint pathway. [Mol Cancer Ther 2007;6(5):1501–8]

Introduction

Benzo[*c*]phenanthridine alkaloids are a family of compounds that were first isolated from plants of Papaveraceae and Rutaceae (1). Natural benzo[*c*]phenanthridine alkaloids such as nitidine and fagaronine were known for their antileukemic activities as early as in the 1970s (2, 3). Fagaronine has been reported to be a DNA binding agent and inhibitor of topoisomerases (4, 5). Nitidine has also been reported to be a topoisomerase I inhibitor (6). However, neither of these compounds was developed as an anticancer drug because of low potency. A synthetic derivative NK109 (7), which was developed by Nippon Kayaku Co. Ltd., was described as a topoisomerase II inhibitor (8) and showed *in vitro* and *in vivo* cytotoxic activity against a range of human tumors (9), but it failed to exhibit clinical activity. Further study showed that NK109 was reduced to an inactive metabolite *in vivo*. To overcome this route of metabolic elimination, NK314 was synthesized by introducing a trimethylene group to N_5-C_6 of NK109 (ref. 10; Fig. 1A). NK314 has shown strong antitumor activities in gastric, colon, lung, and pancreatic cancer xenograft models. Its effectiveness against tumor cell lines resistant to paclitaxel, cisplatin, and irinotecan (11) provided additional rationale for ongoing clinical trials in Japan.

The antitumor mechanism and cellular responses to NK314 have not been characterized. Our present investigations focus on the cell cycle effects, induction of DNA damage, and topoisomerase II inhibitory activity of NK314.

Materials and Methods

Cell Culture

ML-1, a human acute myelogenous leukemia cell line containing wild-type p53, was a gift from Dr. Michael B. Kastan (St. Jude Children's Research Hospital, Memphis, TN). Cells were maintained in exponential growth phase in RPMI 1640 supplemented with 10% fetal bovine serum at 37°C in a humidified atmosphere with 5% CO_2. The population doubling time of ML-1 was 22 to 24 h. Other hematologic cell lines (CCRF-CEM, K562, Raji, and HL60) were cultured under the same condition as ML-1. HeLa cells were cultured in DMEM supplemented with 10% fetal bovine serum. CEM/VM1 cells, which were selected for resistance to teniposide and exhibit cross-resistance to etoposide, were kindly provided by Dr. William T. Beck

Received 12/15/06; revised 3/2/07; accepted 3/26/07.

Grant support: Grants CA28596 and CA32839 and Cancer Center Support grant P30 CA55164 from the National Cancer Institute, Department of Health and Human Services.

The costs of publication of this article were defrayed in part by the payment of page charges. This article must therefore be hereby marked *advertisement* in accordance with 18 U.S.C. Section 1734 solely to indicate this fact.

Requests for reprints: William Plunkett, Department of Experimental Therapeutics, Box 71, The University of Texas M. D. Anderson Cancer Center, 1515 Holcombe Boulevard, Houston, TX 77030.
Phone: 713-792-3335; Fax: 713-794-4316.
E-mail: wplunket@mdanderson.org

doi:10.1158/1535-7163.MCT-06-0780

A

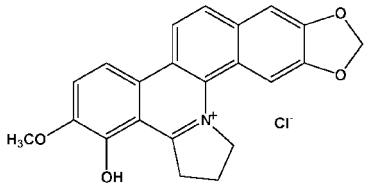

B

Cell line	Origin	p53	Percentage of total cells in G2/M phase at 24 hr	
			Exponentially growing	100 nM NK314 treated
ML-1	AML	Wild type	22	85
CCRF-CEM	T-ALL	Mutant	26	89
K-562	CML	Mutant	26	91
HL-60	AML	Null	24	95
Raji	Lymphoma	Mutant	28	89
Hela	Cervical Cancer	Low level	29	86

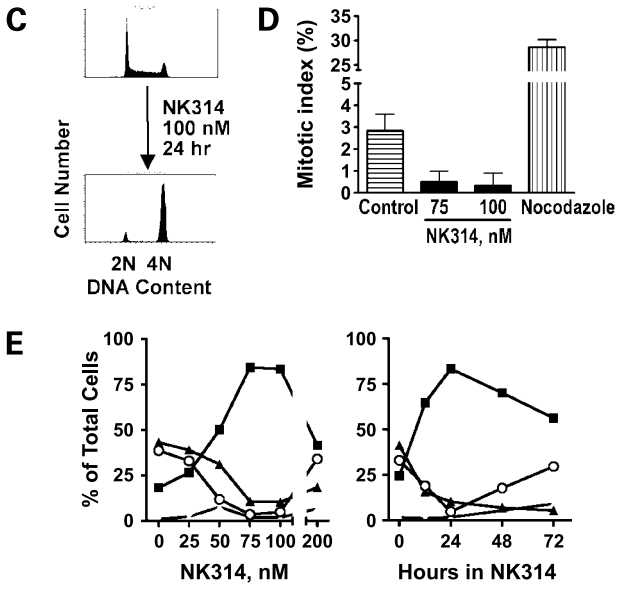

Figure 1. Structure of NK314 and cell cycle action of NK314 in human cancer cell lines. **A,** chemical structure of NK314. **B,** cancer cell lines of diverse origins were treated with 100 nmol/L NK314 for 24 h. DNA content was analyzed by propidium iodide staining and flow cytometry. **C,** ML-1 cells were treated with NK314 and significant G_2-M arrest was shown by propidium iodide staining. **D,** the number of mitotic cells was counted in control, NK314-treated (75 and 100 nmol/L), and nocodazole-treated (400 ng/mL) cells. The treatment time was 24 h. The mitotic index is the percentage of mitotic cells in the total population. **E,** ML-1 cells were treated with various concentrations of NK314 for 24 h (*left*) or 100 nmol/L NK314 for 3 d (*right*; ■, G_2-M; ▲, G_1; ○, S; ×, sub-G_1). *Points,* mean of two identical experiments.

(12). CEM/C2 cells, selected for resistance to camptothecin (13, 14), were purchased from American Type Culture Collection (ATCC CRL-2264). All cells were free of *Mycoplasma* as determined by an ELISA kit (Life Technologies MycoTest kit).

Chemicals and Antibodies

NK314 was provided by Nippon Kayaku Co. Ltd. A stock solution (20 mmol/L) was prepared in 5% glucose solution, sterilized by filtration, stored at −70°C, and diluted in sterile 5% glucose solution just before use. 7-Hydroxystaurosporine (UCN-01, NSC 638850) was provided by the Drug Synthesis and Chemistry Branch, Division of Cancer Treatment, National Cancer Institute (Bethesda, MD). Aliquots of UCN-01 were stored at 10 mmol/L in DMSO at −20°C and diluted in serum-free medium immediately before each experiment. All other chemicals were reagent grade. Sources of antibodies are as follows: rabbit polyclonal antibodies against phospho-Ser^{317} of Chk1, phospho-Ser^{216} of Cdc25C, phospho-Tyr^{15} of Cdk1, phospho-Ser^{15} of p53 (Cell Signaling Technology), mouse monoclonal antibody against p53 (Oncogene Research Products), rabbit anti-Chk1, mouse anti-Cdk1, mouse anti-p21 (Santa Cruz Biotechnology), mouse monoclonal antibodies against Cdc25C, phospho-Ser^{139} of H2AX (Upstate Biotechnology), mouse monoclonal antibodies against β-actin (Sigma-Aldrich), antimouse or antirabbit immunoglobulin G horseradish peroxidase–conjugated antibody (Amersham Biosciences), IRDye 680 goat anti-mouse or IRDye 800CW goat anti-rabbit immunoglobulin G (Li-Cor, Inc.).

Cell Cycle Analysis

Cells were washed with ice-cold PBS (pH 7.4) and fixed in 70% ethanol. Fixed cells were washed with PBS before incubation with 50 μg/mL propidium iodide (Sigma-Aldrich) and 2.5 μg/mL DNase-free RNase A (Roche). Fluorescence was measured on a Becton Dickinson FACSCalibur flow cytometer. At least 20,000 cells were measured for each sample.

Quantification of Mitotic Index

After centrifugation of cells to slides by Cytospin (Thermo Electron Corp.), cells were fixed with 4% paraformaldehyde in PBS (pH 7.4) and mounted in Vectashield mounting medium with 1.5 μg/mL 4′,6-diamidino-2-phenylindole (Vector Laboratories). Mitotic morphology was identified by the appearance of nuclear DNA condensation by epifluorescence microscopy (Nikon). At least 200 cells per field in a minimum of three randomly selected fields were counted on three slides for each sample.

Clonogenic Assays

Cells were incubated with indicated concentrations of drug for a doubling time, washed into fresh medium, and dilutions of 500 to 10,000 cells were plated in 35-mm plastic dishes containing MethoCult H4230 methylcellulose medium (Stem Cell Technologies). Colonies of 10 to 200 cells were counted with the aid of a dissecting microscope after 8 doubling times. The plating efficiency of untreated controls was 30% to 50%. Values are the mean ± SD of at least triplicate plates.

Immunoblotting

Cells pellets were washed with ice-cold PBS and lysed at 4°C by sonication in radioimmunoprecipitation assay buffer [PBS containing 1% NP40, 0.5% sodium deoxycholate, 0.1% SDS, 1 mmol/L EDTA (pH 8), 1 mmol/L sodium orthovanadate (pH 10), 50 mmol/L NaF, 10 mmol/L

β-glycerophosphate, 20 μg/mL aprotinin, 10 μg/mL leupeptin, 10 μg/mL pepstatin, 2 mmol/L phenylmethylsulfonyl fluoride]. Lysates were centrifuged at 14,000 rpm for 10 min, and the supernatants were subjected to protein content determination using a detergent-compatible protein assay kit (Bio-Rad) according to the manufacturer's instructions. An equal volume of 2× SDS sample loading buffer containing 100 mmol/L Tris-HCl (pH 6.8), 10% glycerol, 4% SDS, 0.05% bromophenol blue, and 5% β-mercaptoethanol was added to cell lysates before heating at 95°C to 100°C for 5 min. Aliquots of 40 to 50 μg total cell protein were loaded onto 10% SDS-polyacrylamide gels. Proteins were separated by electrophoresis at constant voltage (80–200 V) and electrotransferred to nitrocellulose membranes at 150 mA overnight at 4°C. Membranes were blocked at room temperature for 1 h in TBS/0.05% Tween 20 (pH 7.4) containing 5% nonfat dried milk and incubated with primary antibodies overnight at 4°C. Membranes were washed with TBS/0.05% Tween 20 thrice and incubated with secondary antibodies conjugated to horseradish peroxidase for 1 h. After washing thrice, the blots were visualized by enhanced chemiluminescence according to the manufacturer's instructions (Pierce). Some membranes were incubated with IR dye secondary antibodies and visualized by Li-Cor Odyssey Imager (Li-Cor).

Immunofluorescent Detection of γ-H2AX

γ-H2AX was detected by flow cytometry. Ethanol-fixed cells were permeabilized with 0.5% Triton X-100 in PBS. After centrifugation, the cell pellet was incubated in 100-μL PBS containing 1% bovine serum albumin and 7.5 μg of a monoclonal antibody specifically recognizing phospho-Ser^{139} on histone H2AX at room temperature. After being washed with PBS containing 1% bovine serum albumin, cells were incubated with FITC-conjugated goat anti-mouse immunoglobulin G antibody (Jackson ImmunoResearch Laboratories, Inc.) diluted at a ratio of 1:60 in the dark. The cells were washed again and then incubated with PBS containing propidium iodide and RNase A before the fluorescence was measured by flow cytometry. γ-H2AX was also detected by confocal microscopy. Cells were centrifuged onto slides, fixed in 4% paraformaldehyde, and permeabilized with 0.5% Triton X-100. After blocking with PBS containing 6% goat serum (ICN Biochemicals, Inc.), cells were incubated with γ-H2AX (phospho-Ser^{139}) antibody at 500-fold dilution in 3% goat serum in PBS for 2 h followed by three washes with PBS containing 0.1% NP40. Then, cells were incubated for 1 h with a FITC-conjugated goat anti-mouse immunoglobulin G antibody diluted at a ratio of 1:100 followed by three washes. Cell nuclei were stained in PBS with propidium iodide and RNase. The slides were mounted with mounting medium Vectashield (Vector Laboratories) and sealed with nail polish. γ-H2AX and nuclear staining were viewed with a Olympus FV500 Confocal Laser Scanning Microscope (Olympus) using a 60× objective.

Cytogenetic Analysis

Colcemid (100 ng/mL) was added to cell cultures 2 h before harvesting. Cells were resuspended and swollen in 0.075 mol/L KCl at 37°C for 10 min before being fixed in fresh methanol/acetic acid (3:1, v/v) at room temperature for 20 min. Following three washes with ice-cold methanol/acetic acid (3:1, v/v), fixed cells were spread onto Superfrost microscopic slides (Erie Scientific) and air-dried overnight. Spreads were stained with 4% (v/v) Giemsa (Karyomax Giemsa stock solution, Invitrogen Corp.) freshly prepared in Gurr buffer (Invitrogen) at room temperature for 20 min. Following rinsing with Millipore water, stained slides were air-dried overnight before mounting using Eukitt Histomount (Zymed Laboratories, Inc.). All slides were blinded before quantitation of chromosomal aberrations (including gaps and breaks) by microscopic examination. At least 60 metaphase spreads were analyzed on three separate slides for each sample. For each treatment, variations between slides were not remarkable as determined by statistical assays (data not shown).

Topoisomerase II Assays

Inhibition of topoisomerase II activity by NK314 was measured by a supercoiled DNA relaxation assay using a topoisomerase II drug screening kit (TopoGEN). Briefly, 0.25 μg supercoiled DNA (pRYG) was suspended in a reaction buffer [50 mmol/L Tris-HCl (pH 8.0), 120 mmol/L KCl, 10 mmol/L $MgCl_2$, 0.5 mmol/L DTT, 0.5 mmol/L ATP]. Drug was added to the mixture before the reaction was started by topoisomerase II enzyme addition. After a 30-min incubation at 37°C, the reaction was stopped by adding 0.1 volume of 10% SDS. The DNA-bound protein (topoisomerase II) was digested by proteinase K (50 μg/mL) at 37°C for 15 min. The proteinase K was removed by chloroform/isoamyl alcohol (24:1, v/v) treatment. DNA samples were then analyzed by 1% agarose gel electrophoresis. The gel did not contain ethidium bromide and was stained by 0.5 μg/mL ethidium bromide before UV photography. The stabilization of topoisomerase II cleavage complex was studied by using pBR322 plasmid, instead of pRYG, and 1% agarose gel containing 0.5 μg/mL ethidium bromide. The other procedures were the same as the relaxation assay.

Results

G_2 Arrest Is Induced by NK314

The effect of NK314 on cell cycle progression was determined after incubation of six different cell lines with the compound for at least a population doubling time (Fig. 1B). DNA content analysis showed that >85% of the total population of each line was arrested at G_2-M phase after a 24-h incubation with 100 nmol/L NK314, regardless of the p53 status of the cells. Incubation with this concentration did not induce cell lysis, as there was no increase of cells with a sub-G_1 DNA content. To characterize the NK314-induced G_2-M arrest in greater detail, we focused our investigations on ML-1 human acute myeloid leukemia cells. ML-1 cells were arrested significantly at G_2-M phase after 24-h incubation with 100 nmol/L NK314 (Fig. 1C). To distinguish G_2 cells from mitotic cells, we conducted microscopic evaluation, which showed fewer

mitotic figures in NK314-treated cultures (<1%) than that in either controls (3%; $P = 0.01$) or nocodazole-treated cultures (30%; $P < 0.01$), indicating that these cells were arrested at G_2 (Fig. 1D). To define the concentration dependency of NK314-induced G_2 arrest in ML-1 cells, cells were incubated for 24 h with different concentrations of NK314 (Fig. 1E, *left*). Maximum G_2 accumulations, increasing from 22% to 85%, were achieved with 75 to 100 nmol/L NK314. Cell lysis was not evident as cells with a sub-G_1 DNA content were <10%. To determine the time dependency of NK314-induced G_2 arrest, ML-1 cells were exposed to 100 nmol/L NK314 for 3 days (Fig. 1E, *right*). The population with a G_2 DNA content peaked at 24 h, approximately the time required for the population to double, and the arrest was considerably sustained for 72 h.

NK314 Activates the Chk1-Cdc25C-Cdk1 Checkpoint Signaling Pathway

To elucidate the molecular basis of NK314-induced G_2 arrest, we first investigated the activation of the Chk1-Cdc25C-Cdk1 G_2 checkpoint pathway. On incubation of ML-1 cells with 100 nmol/L NK314, the DNA damage checkpoint kinase Chk1 became phosphorylated on Ser^{317} within 6 h, indicating its activation by upstream sensors (Fig. 2). This was associated with phosphorylation of the Chk1 target protein Cdc25C on Ser^{216}, consistent with the inhibitory regulation of its phosphatase activity. Thus, Cdk1 accumulated in a Tyr^{15}-phosphorylated state. These changes indicate G_2 checkpoint activation. In addition, phosphorylation of Ser^{15} on p53 was evident by 6 h after NK314 treatment. This was associated with the induction of p21 by 6 h and an increase in total p53 by 24 h. However, the activation of p21 may not be required for the NK314-induced G_2 arrest because p53 null or mutant cells were also arrested by NK314 (Fig. 1B).

NK314 Causes DNA Double-Strand Breaks in ML-1 Cells

The histone variant H2AX is phosphorylated rapidly on Ser^{139} (γ-H2AX) in response to DNA double-strand breaks (15). Immunoblotting showed the induction of γ-H2AX in ML-1 cells treated with 100 nmol/L NK314 at 24 h but not at 1 h (Fig. 3A). Flow cytometry showed small portions of the population to be γ-H2AX positive at 1 and 12 h, a response that was associated predominantly with cells with G_2 DNA content. H2AX became phosphorylated in 59% of the total cells in response to 100 nmol/L NK314 within 24 h with 96% of the γ-H2AX–positive cells in the G_2 population (Fig. 3B). Furthermore, NK314 at 200 nmol/L or greater concentrations induced extensive γ-H2AX formation after only 1-h exposure to NK314, indicating a steep concentration response in the 100 to 200 nmol/L range, with >95% of cells being γ-H2AX positive in response to >400 nmol/L NK314 (Fig. 3C). However, these were distributed in all cell cycle phases. To determine if NK314-induced H2AX phosphorylation was a result of apoptosis (16), cells were stained with Annexin V and propidium iodide. No evidence of apoptosis was found either at 24 h with 100 nmol/L NK314 or at 1 h with 100 to 1,000 nmol/L NK314 (data not shown), a result that is consistent with the lack of cells with a sub-G_1 DNA content. Confocal microscopy also showed the formation of γ-H2AX foci in the nuclei of ML-1 cells in response to NK314 (Fig. 3D). Consistent with the flow cytometric results, the intensity of γ-H2AX foci in cells treated with 1,000 nmol/L NK314 for 1 h was greater than that in cells treated with 100 nmol/L NK314 for 24 h.

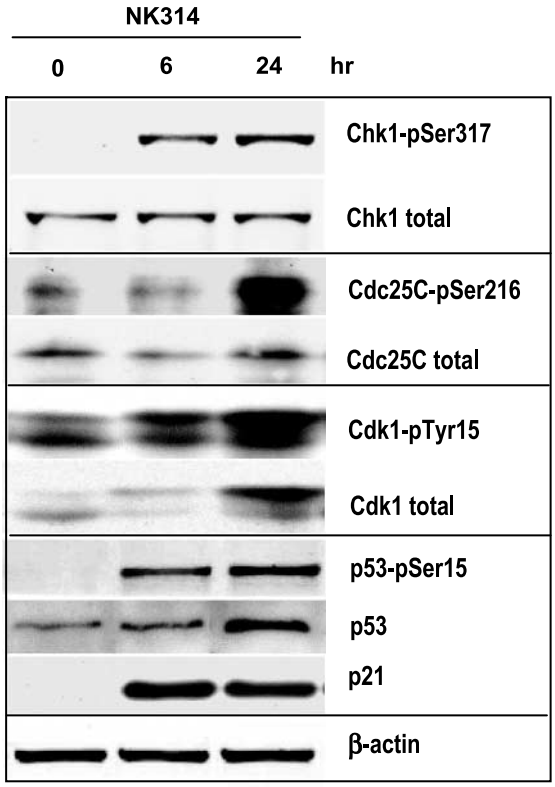

Figure 2. Activation of the checkpoint signals in response to NK314. Exponentially growing ML-1 cells were incubated with 100 nmol/L NK314 for 24 h. Equal amounts of cell lysate proteins were subjected to immunoblot analysis with indicated antibodies. β-Actin was used for a loading control for all assays.

Based on these results, we hypothesized that NK314 treatment may lead to formation of double-strand breaks. To test this postulate, we conducted cytogenetic analysis on ML-1 cells collected in metaphase with colcemid. Because few mitotic cells were evident after NK314 treatment, a Chk1 kinase inhibitor, UCN-01, was used to abrogate NK314-induced G_2 arrest (17–21). As a control for this study, cells arrested in G_2 with 100 nmol/L NK314 were exposed to 100 nmol/L UCN-01. This resulted in a rapid decline in the G_2 population from ~70% to only 10% in 12 h, whereas 60% of cells treated with NK314 alone remained in G_2 (Supplementary Fig. S1).[4] This was accompanied by cells proceeding through mitosis and an abrupt increase of cells in G_1. In contrast, treatment of ML-1 cells with 100 nmol/L UCN-01 alone had no discernible effect on population doubling time

[4] Supplementary data for this article are available at Molecular Cancer Therapeutics Online (http://mct.aacrjournals.org/).

or cell cycle distribution (21). To evaluate the ability of NK314 to cause chromosome aberrations, NK314-arrested cells were treated with UCN-01 for 6 h in the presence of colcemid. Because UCN-01 abrogates the G_2 checkpoint, it allows NK314-arrested cells to progress to mitosis and colcemid arrests cells at mitosis. This provides an opportunity to visualize chromosome abnormalities (Fig. 4A). By scoring 210 well-resolved metaphases, we detected an average of five chromatid type aberrations per cell, including gaps and breaks (Fig. 4B). In contrast, there were fewer aberrations found in either control (mock-treated) cells (0.05 per cell; $P < 0.01$) or cells treated with UCN-01 alone (0.1 per cell; $P < 0.01$; data not shown). ML-1 cells are pseudotetraploid with a mean of 90 chromosomes (21).

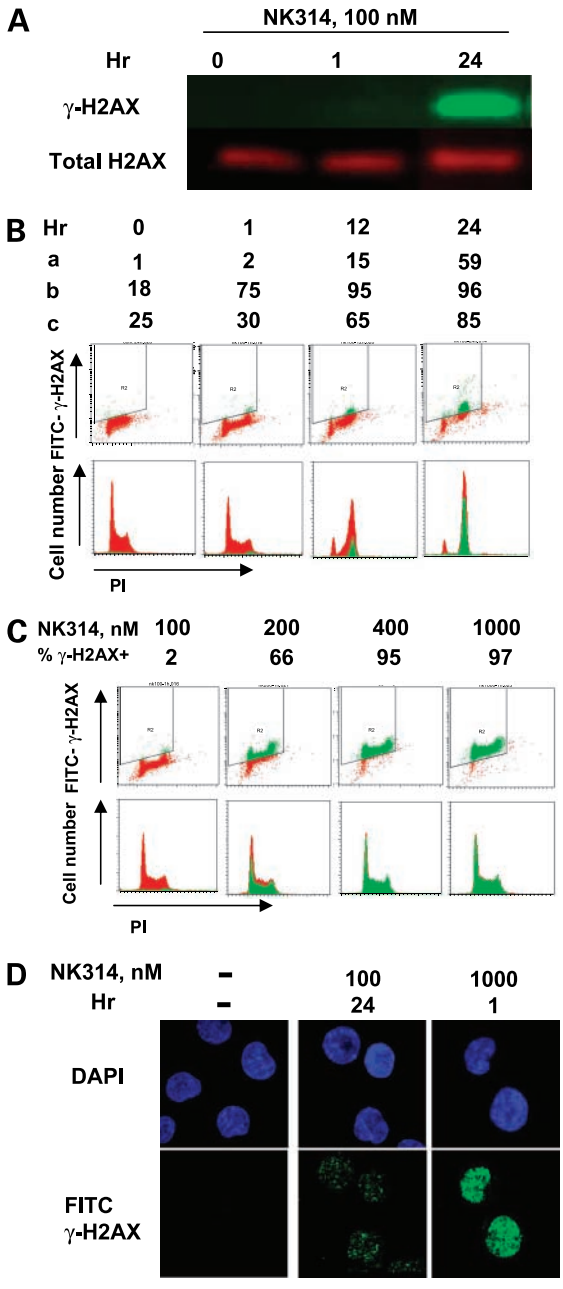

Figure 3. Histone H2AX phosphorylation caused by NK314. **A,** ML-1 cells were incubated with 100 nmol/L NK314 for 24 h and samples were collected at 0, 1, and 24 h to detect γ-H2AX by immunoblotting. **B,** ML-1 cells were incubated with 100 nmol/L NK314 for 24 h when cells were fixed and stained by Ser^{139}-phosphorylated H2AX (γ-H2AX). **C,** ML-1 cells were incubated with 100, 200, 400, or 1,000 nmol/L NK314 for 1 h and γ-H2AX was determined by flow cytometry. *a,* percentage of γ-H2AX-positive cells in total cells. *b,* percentage of γ-H2AX positive G_2 cells in total γ-H2AX positive cells. *c,* percentage of G_2 cells in total cells. **D,** ML-1 cells were stained by FITC-labeled γ-H2AX antibody and representative images were taken by confocal microscopy.

NK314 Targets Topoisomerase IIα

Other benzo[*c*]phenanthridine compounds were reported to be inhibitors of topoisomerases (5, 8, 22). Therefore, we tested the topoisomerase II inhibitory activity of NK314. In a cell-free topoisomerase II relaxation assay, 4 to 8 μmol/L NK314 or 80 to 160 μmol/L etoposide inhibited the relaxation of supercoiled plasmid DNA by topoisomerase IIα (Fig. 5A), indicating that NK314 is a more potent topoisomerase IIα inhibitor than etoposide. To test if NK314 traps topoisomerase IIα in its DNA cleavage complex form, we used the pBR322 plasmid as supercoiled DNA substrate and detected linear DNA formation, which indicates the stabilization of cleavage complexes (23). This was evident at NK314 concentrations between 4 and 8 μmol/L, again indicating that NK314 is considerably more potent than etoposide, which poisoned the enzyme at 80 to 160 μmol/L (Fig. 5B). To study if NK314 inhibits topoisomerases in growing cells, we studied cell lines that express mutated enzymes. CEM/VM1 cells have a mutant topoisomerase IIα that causes resistance to topoisomerase II inhibitors such as etoposide, teniposide, and doxorubicin (24). CEM/C2 cells have a mutant topoisomerase I that causes resistance to the topoisomerase I inhibitor camptothecin (13, 14). Clonogenic assays showed that CEM/VM1 cells were 20 times more resistant to NK314 compared with parental CEM cells. In contrast, CEM/C2 cells retained full sensitivity to NK314. CEM/VM1 cells were also 100 times more resistant to etoposide, and CEM/C2 cells were 1,000 times more resistant to camptothecin (Fig. 5C). These results suggest that topoisomerase IIα is a major intracellular target of NK314. Finally, to compare the cytotoxicity of NK314 with etoposide, clonogenic assays conducted with CEM cells showed that the IC_{90} values of NK314 and etoposide were 55 and 260 nmol/L, respectively (Fig. 5D). Thus, NK314 is more potent than etoposide in CEM cells, which is consistent with the potency of the inhibition of topoisomerase IIα *in vitro* by these drugs.

Discussion

Our findings support the conclusion that the dominant mechanism of NK314 action is the inhibition of topoisomerase IIα, which generates cell cycle perturbations and cytotoxicity. NK314 directly inhibited supercoiled DNA relaxation by topoisomerase IIα. Topoisomerase IIα mutant CEM/VM1 cells, but not topoisomerase I mutant CEM/C2 cells, were cross-resistant to NK314. Double-strand DNA breaks were also visualized as chromosomal

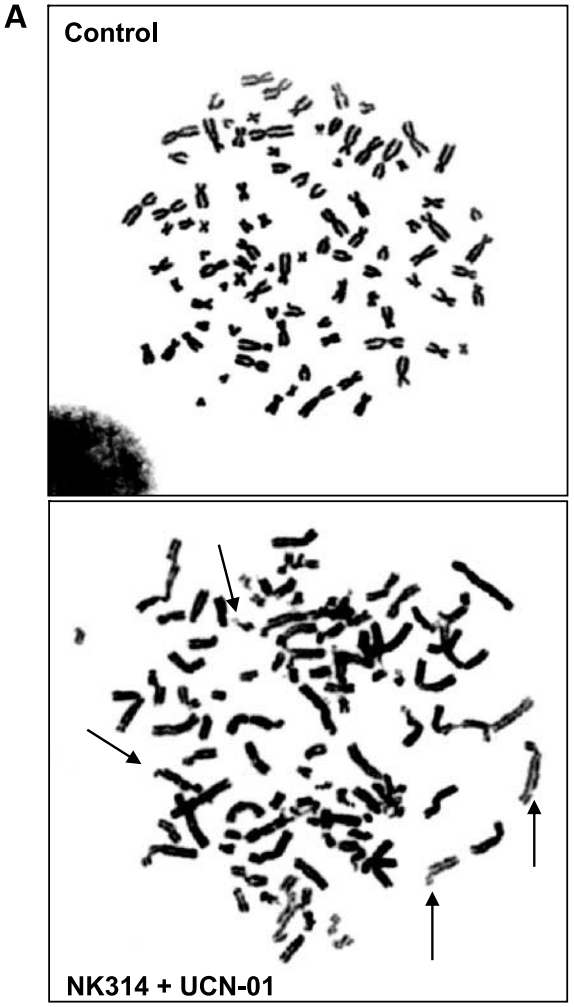

B

	Control	UCN-01 alone	NK314 + UCN-01
Cells scored	240	210	210
Chromosomal aberrations	12	20	1050
Aberrations per cell	0.05 ± 0.24	0.10 ± 0.31#	5.00 ± 1.80*

* $p < 0.01$ vs Control or UCN-01 alone;
\# $p = 0.09$ vs Control.

Figure 4. Chromosome aberrations induced by NK314. Cells were treated with 100 nmol/L NK314 for 24 h and 100 nmol/L UCN-01 was added for another 6 h to abrogate the G_2 arrest before sample collection. **A,** representative images of chromosome spreads were taken. *Arrows,* chromosome breaks. **B,** quantitation and comparison of chromosome aberrations.

aberrations when the G_2 checkpoint of NK314-arrested cells was abrogated by UCN-01. NK314 treatment was associated with the phosphorylation of H2AX, an action that was predominant in the G_2 population. This suggests that activation of the Chk1-Cdc25C-Cdk1–mediated G_2 checkpoint pathway was a response to double-strand DNA breaks.

The topoisomerase II relaxation assays showed that 8 μmol/L NK314 or 160 μmol/L etoposide inhibited the relaxation of supercoiled plasmid DNA by topoisomerase IIα and trapped topoisomerase IIα in cleavage complexes (Fig. 5A and B), indicating that NK314 is a more potent topoisomerase IIα inhibitor than etoposide. The concentrations required for NK314 (75 nmol/L) and etoposide (400 nmol/L) to maximally arrest ML-1 cells are 100 times

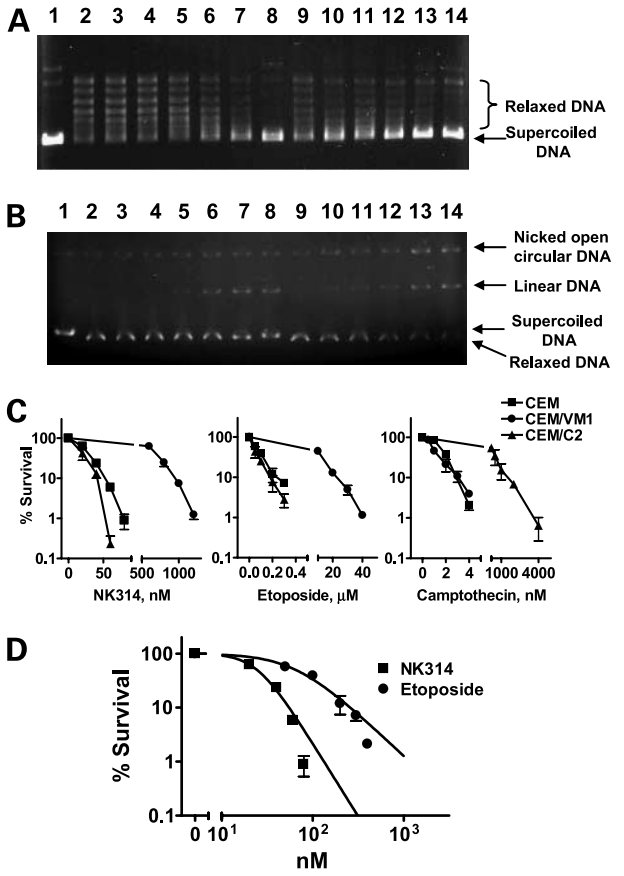

Figure 5. Action of NK314 on topoisomerase IIα and cytotoxicity of NK314. **A,** supercoiled plasmid DNA (pRYG) was incubated with topoisomerase IIα and various concentrations of NK314 or etoposide. The reaction products were separated in 1% agarose gel without ethidium bromide. *Lane 1,* pRYG; *lane 2,* pRYG and topoisomerase IIα (no drug control); *lanes 3* to *8,* pRYG and topoisomerase IIα in the presence of 0 (solvent control), 0.5, 1, 2, 4, and 8 μmol/L NK314; *lanes 9* to *14,* pRYG and topoisomerase IIα in the presence of 0 (solvent control), 10, 20, 40, 80, and 160 μmol/L etoposide. **B,** supercoiled plasmid DNA (pBR322) was incubated with topoisomerase IIα and various concentrations of NK314 or etoposide. The reaction products were separated in 1% agarose gel with 0.5 μg/mL ethidium bromide. *Lane 1,* pBR322; *lane 2,* pBR322 and topoisomerase IIα (no drug control); *lanes 3* to *8,* pBR322 and topoisomerase IIα in the presence of 0 (solvent control), 2, 4, 8, 16, and 32 μmol/L NK314; *lanes 9* to *14,* pBR322 and topoisomerase IIα in the presence of 0 (solvent control), 20, 40, 80, 160, and 320 μmol/L etoposide. **C,** CEM, CEM/VM1 (etoposide resistant), and CEM/C2 (camptothecin resistant) cells were incubated with various concentrations of NK314, etoposide, and camptothecin for a doubling time and plated in methylcellulose. Colonies were counted after 8 doubling times (■, CEM; ●, CEM/VM1; ▲, CEM/C2). **D,** CEM cells were incubated with various concentrations of NK314 (■) or etoposide (●) for 24 h and plated in methylcellulose. Colonies were counted after 8 d.

less than those needed for the cell-free topoisomerase II relaxation assay. One reason may be that the DNA damage threshold to evoke checkpoint response is far less than that which can be detected by relaxation of supercoiled DNA by topoisomerase IIα in this cell-free assay. In addition, the cell-free assay generates nearly total conversion of the plasmid substrate, whereas fewer lesions may be detected by the checkpoint sensors (Fig. 4).

CEM/VM1 cells, which are resistant to etoposide due to expression of mutant topoisomerase IIα (25, 26), and CEM/C2 cells, which are resistant to camptothecin due to expression of mutant topoisomerase I (13, 14), were used to study if topoisomerase IIα is the intracellular target of NK314. The clonogenic assay showed that CEM/VM1 cells were 20 times more resistant to NK314 and 100 times more resistant to etoposide but not resistant to camptothecin compared with CEM cells. However, CEM/C2 cells were 1,000 times more resistant to camptothecin but not resistant to NK314 or etoposide (Fig. 5C). These studies indicate that topoisomerase IIα, not topoisomerase I, is a major target of NK314. Nevertheless, the finding that CEM/VM1 cells are less resistant to NK314 than to etoposide suggests that the mutation does not affect the actions of NK314 as much as it does the effects of etoposide, or there may be other targets of NK314. For instance, another benzo[*c*]phenanthridine alkaloid, sanguinarine, was reported to be an inhibitor of mitogen-activated protein kinase phosphatase-1 (27). Whether NK314 inhibits mitogen-activated protein kinase phosphatase-1 and whether this inhibition leads to antitumor activity need further investigation. There was also evidence that NK314 stabilized topoisomerase IIα-DNA cleavage complex using the *in vivo* complex of enzyme bioassay (28). The effect of NK314 on DNA fragmentation and cytotoxicity was largely inhibited by topoisomerase IIα small interfering RNA but not by topoisomerase IIβ small interfering RNA. NK314-induced DNA fragmentation was inhibited by topoisomerase II catalytic inhibitors ICRF-193 and suramin (28). Together, these results suggest that NK314 is a potent topoisomerase IIα specific inhibitor that stabilizes cleavage complex formation, which results in DNA double-strand breaks.

Cytogenetic analysis showed that cells treated with NK314 and UCN-01 exhibit more chromosome aberrations than either control cells or cells treated with UCN-01 alone (Fig. 4). Few mitotic figures were observed among cells treated with NK314 alone, due to the stringent G_2 checkpoint, precluding statistical comparison with the UCN-01–treated population. Considering that UCN-01 alone did not contribute to the generation of chromosome aberrations and that γ-H2AX was positive in ML-1 cells treated with NK314 alone, we conclude that the abrogation of the G_2 checkpoint by UCN-01 facilitated premature chromosome condensation, which permitted visualization of DNA double-strand breaks induced by NK314. Separate investigations have also reported that pulse-field gel electrophoresis and neutral filter elution assays also showed that NK314 induced DNA double-strand breaks (11). Thus, it is likely that cells respond to the double-strand breaks generated by NK314 inhibition of topoisomerase IIα by activating the G_2 cell cycle checkpoint pathway.

The rapid phosphorylation of H2AX by upstream DNA damage sensors, such as ataxia telangiectasia mutated (ATM) and ataxia telangiectasia mutated and Rad3-related (ATR), in response to DNA double-strand breaks is well documented (15, 29, 30). Thus, the G_2 arrest induced by 100 nmol/L NK314 is likely to result from DNA double-strand breaks, as 95% of the γ-H2AX–positive cells were in the G_2 population following a 12-h incubation with NK314 (Fig. 3B), indicating that γ-H2AX–positive cells accumulated in the G_2 phase. Whereas maximal accumulation of γ-H2AX can be achieved in 10 min in response to DNA double-strand breaks caused by ionizing radiation (15), 100 nmol/L NK314 did not induce significant γ-H2AX formation in 1 h. This suggests that the threshold to relay DNA damage signal to activate the G_2 checkpoint is lower than that required to induce γ-H2AX formation to facilitate DNA repair. However, >200 nmol/L NK314 induced extensive γ-H2AX formation in 1 h, regardless of cell cycle phase (Fig. 3C). This suggests that the NK314-induced DNA double-strand breaks were not a consequence of replication of damaged DNA during a 1-h experience but raises the possibility that different targets are affected by NK314 concentrations greater than 200 nmol/L. The lack of cell cycle specificity at greater NK314 concentrations is similar to that caused by ionizing radiation or the radiomimetic agent bleomycin (31). However, this differs from the topoisomerase I inhibitor camptothecin-induced γ-H2AX formation, which is largely restricted in S phase, presumably because double-strand breaks are caused by collision of replication forks with the stabilized cleavage complexes (32).

Molecular pharmacology studies in ML-1 cells indicated an activation of the Chk1-Cdc25C-Cdk1 pathway. Although p53 became phosphorylated on Ser^{15} and expression of p21 increased in response to NK314 in p53 wild-type ML-1 cells, cells lacking functional p53 [CCRF-CEM (33), Raji (34), K562 (35), and HL60 (36)] were also arrested in response to NK314 (Fig. 1B), suggesting that p53 and p21 are not required in the onset of G_2 checkpoint activation. Nevertheless, these regulators have been shown to be required to enforce G_2 arrest after DNA damage (37). Their actions may have sustained the NK314-induced G_2 arrest for 72 h in p53 wild-type ML-1 cells (Fig. 1E). As the G_2 cell cycle arrest is thought to function as a defense mechanism in response to DNA damage, which allows cells to repair DNA damage before moving to mitosis (38), NK314 may induce DNA damage as do other benzo[*c*]phenanthridines such as fagaronine, nitidine, and NK109 (5, 6, 8). Although there have been no reports on the cell cycle effect of these compounds, inhibitors of topoisomerase II such as etoposide and doxorubicin induce G_2 arrest in cells (39, 40) including those lines that we tested.

Acknowledgments

We thank Dr. William T. Beck (Department of Biopharmaceutical Sciences, University of Illinois at Chicago, Chicago, IL) for kindly providing the CEM/VM1 cells, and Dr. Walter Hittelman (Department of Experimental Therapeutics, The University of Texas M. D. Anderson Cancer Center, Houston, TX) for critical discussion and assistance with the cytogenetic analyses.

References

1. Ishii H, Ishikawa T. [Chemistry of benzo[*c*]phenanthridine alkaloids having antineoplastic activity (author's transl)]. Yakugaku Zasshi 1981; 101:663 – 87.

2. Messmer WM, Tin-Wa M, Fong HH, et al. Fagaronine, a new tumor inhibitor isolated from *Fagara zanthoxyloides* Lam. (Rutaceae). J Pharm Sci 1972;61:1858 – 9.

3. Cheng CC, Engle RR, Hodgson JR, et al. Absence of mutagenicity of coralyne and related antileukemic agents: structural comparison with the potent carcinogen 7,12-dimethylbenz[*a*]anthracene. J Pharm Sci 1977; 66:1781 – 3.

4. Fleury F, Sukhanova A, Ianoul A, et al. Molecular determinants of site-specific inhibition of human DNA topoisomerase I by fagaronine and ethoxidine. Relation to DNA binding. J Biol Chem 2000;275:3501 – 9.

5. Larsen AK, Grondard L, Couprie J, et al. The antileukemic alkaloid fagaronine is an inhibitor of DNA topoisomerases I and II. Biochem Pharmacol 1993;46:1403 – 12.

6. Wang LK, Johnson RK, Hecht SM. Inhibition of topoisomerase I function by nitidine and fagaronine. Chem Res Toxicol 1993;6:813 – 8.

7. Nakanishi T, Suzuki M, Saimoto A, Kabasawa T. Structural considerations of NK109, an antitumor benzo[*c*]phenanthridine alkaloid. J Nat Prod 1999;62:864 – 7.

8. Fukuda M, Inomata M, Nishio K, et al. A topoisomerase II inhibitor, NK109, induces DNA single- and double-strand breaks and apoptosis. Jpn J Cancer Res 1996;87:1086 – 91.

9. Kanzawa F, Nishio K, Ishida T, et al. Antitumour activities of a new benzo[*c*]phenanthridine agent, 2,3-(methylenedioxy)-5-methyl-7-hydroxy-8-methoxybenzo[*c*]phenanthridinium hydrogen sulphate dihydrate (NK109), against several drug-resistant human tumour cell lines. Br J Cancer 1997;76:571 – 81.

10. Nakanishi T, Masuda A, Suwa M, et al. Synthesis of derivatives of NK109, 7-OH benzo[*c*]phenanthridine alkaloid, and evaluation of their cytotoxicities and reduction-resistant properties. Bioorg Med Chem Lett 2000;10:2321 – 3.

11. Okamoto K, Seno C, Onda T, Toyoda E, Nishikawa K. Rapid DNA breakage induced by a novel antitumor agent, NK314 [abstract #1368]. Proc Am Assoc Cancer Res 2005;46:319 – b.

12. Bugg BY, Danks MK, Beck WT, Suttle DP. Expression of a mutant DNA topoisomerase II in CCRF-CEM human leukemic cells selected for resistance to teniposide. Proc Natl Acad Sci U S A 1991;88:7654 – 8.

13. Kapoor R, Slade DL, Fujimori A, Pommier Y, Harker WG. Altered topoisomerase I expression in two subclones of human CEM leukemia selected for resistance to camptothecin. Oncol Res 1995;7:83 – 95.

14. Fujimori A, Harker WG, Kohlhagen G, Hoki Y, Pommier Y. Mutation at the catalytic site of topoisomerase I in CEM/C2, a human leukemia cell line resistant to camptothecin. Cancer Res 1995;55:1339 – 46.

15. Rogakou EP, Pilch DR, Orr AH, Ivanova VS, Bonner WM. DNA double-stranded breaks induce histone H2AX phosphorylation on serine 139. J Biol Chem 1998;273:5858 – 68.

16. Rogakou EP, Nieves-Neira W, Boon C, Pommier Y, Bonner WM. Initiation of DNA fragmentation during apoptosis induces phosphorylation of H2AX histone at serine 139. J Biol Chem 2000;275:9390 – 5.

17. Graves PR, Yu L, Schwarz JK, et al. The Chk1 protein kinase and the Cdc25C regulatory pathways are targets of the anticancer agent UCN-01. J Biol Chem 2000;275:5600 – 5.

18. Sampath D, Cortes J, Estrov Z, et al. Pharmacodynamics of cytarabine alone and in combination with 7-hydroxystaurosporine (UCN-01) in AML blasts *in vitro* and during a clinical trial. Blood 2006;107: 2517 – 24.

19. Hotte SJ, Oza A, Winquist EW, et al. Phase I trial of UCN-01 in combination with topotecan in patients with advanced solid cancers: a Princess Margaret Hospital Phase II Consortium study. Ann Oncol 2006; 17:334 – 40.

20. Kortmansky J, Shah MA, Kaubisch A, et al. Phase I trial of the cyclin-dependent kinase inhibitor and protein kinase C inhibitor 7-hydroxystaurosporine in combination with fluorouracil in patients with advanced solid tumors. J Clin Oncol 2005;23:1875 – 84.

21. Liu X, Guo Y, Li Y, et al. Molecular basis for G_2 arrest induced by 2′-*C*-cyano-2′-deoxy-1-β-D-arabino-pentofuranosylcytosine and consequences of checkpoint abrogation. Cancer Res 2005;65:6874 – 81.

22. Makhey D, Gatto B, Yu C, et al. Coralyne and related compounds as mammalian topoisomerase I and topoisomerase II poisons. Bioorg Med Chem 1996;4:781 – 91.

23. Gantchev TG, Hunting DJ. The ortho-quinone metabolite of the anticancer drug etoposide (VP-16) is a potent inhibitor of the topoisomerase II/DNA cleavable complex. Mol Pharmacol 1998;53: 422 – 8.

24. Danks MK, Schmidt CA, Cirtain MC, Suttle DP, Beck WT. Altered catalytic activity of and DNA cleavage by DNA topoisomerase II from human leukemic cells selected for resistance to VM-26. Biochemistry 1988;27:8861 – 9.

25. Danks MK, Yalowich JC, Beck WT. Atypical multiple drug resistance in a human leukemic cell line selected for resistance to teniposide (VM-26). Cancer Res 1987;47:1297 – 301.

26. Chen M, Beck WT. Teniposide-resistant CEM cells, which express mutant DNA topoisomerase IIα, when treated with non-complex-stabilizing inhibitors of the enzyme, display no cross-resistance and reveal aberrant functions of the mutant enzyme. Cancer Res 1993;53: 5946 – 53.

27. Vogt A, Tamewitz A, Skoko J, et al. The benzo[*c*]phenanthridine alkaloid, sanguinarine, is a selective, cell-active inhibitor of mitogen-activated protein kinase phosphatase-1. J Biol Chem 2005;280: 19078 – 86.

28. Kagaya S, Toyoda E, Tokunaka K, et al. NK314, a novel antitumor agent, induces rapid double-strand DNA breaks by specific inhibition of topoisomerase IIα [abstract #5525]. Proc Am Assoc Cancer Res 2006; 47:1299 – a.

29. Burma S, Chen BP, Murphy M, Kurimasa A, Chen DJ. ATM phosphorylates histone H2AX in response to DNA double-strand breaks. J Biol Chem 2001;276:42462 – 7.

30. Ward IM, Chen J. Histone H2AX is phosphorylated in an ATR-dependent manner in response to replicational stress. J Biol Chem 2001; 276:47759 – 62.

31. MacPhail SH, Banath JP, Yu Y, Chu E, Olive PL. Cell cycle-dependent expression of phosphorylated histone H2AX: reduced expression in unirradiated but not X-irradiated G_1-phase cells. Radiat Res 2003;159: 759 – 67.

32. Furuta T, Takemura H, Liao ZY, et al. Phosphorylation of histone H2AX and activation of Mre11, Rad50, and Nbs1 in response to replication-dependent DNA double-strand breaks induced by mammalian DNA topoisomerase I cleavage complexes. J Biol Chem 2003;278: 20303 – 12.

33. Cheng J, Haas M. Frequent mutations in the p53 tumor suppressor gene in human leukemia T-cell lines. Mol Cell Biol 1990;10:5502 – 9.

34. Duthu A, Debuire B, Romano J, et al. p53 mutations in Raji cells: characterization and localization relative to other Burkitt's lymphomas. Oncogene 1992;7:2161 – 7.

35. Law JC, Ritke MK, Yalowich JC, Leder GH, Ferrell RE. Mutational inactivation of the p53 gene in the human erythroid leukemic K562 cell line. Leuk Res 1993;17:1045 – 50.

36. Wolf D, Rotter V. Major deletions in the gene encoding the p53 tumor antigen cause lack of p53 expression in HL-60 cells. Proc Natl Acad Sci U S A 1985;82:790 – 4.

37. Bunz F, Dutriaux A, Lengauer C, et al. Requirement for p53 and p21 to sustain G_2 arrest after DNA damage. Science 1998;282: 1497 – 501.

38. Zhou BB, Elledge SJ. The DNA damage response: putting checkpoints in perspective. Nature 2000;408:433 – 9.

39. Kalwinsky DK, Look AT, Ducore J, Fridland A. Effects of the epipodophyllotoxin VP-16-213 on cell cycle traverse, DNA synthesis, and DNA strand size in cultures of human leukemic lymphoblasts. Cancer Res 1983;43:1592 – 7.

40. Barlogie B, Drewinko B, Johnston DA, Freireich EJ. The effect of Adriamycin on the cell cycle traverse of a human lymphoid cell line. Cancer Res 1976;36:1975 – 9.